Ryerson University Digital Commons @ Ryerson

Physics Publications and Research

Physics

1-1-1997

New Acoustic Beams Designed for Rapid Lesion Formation: Limitations Near the Skin During Multiple Lesion Treatments

JW Hunt

AY Xuan

E Seto

AE Worthington

L Chen

See next page for additional authors

Follow this and additional works at: http://digitalcommons.ryerson.ca/physics



Part of the Atomic, Molecular and Optical Physics Commons

Recommended Citation

Hunt, JW; Xuan, AY; Seto, E; Worthington, AE; Chen, L; Kolios, MC; and Sherar, MD, "New Acoustic Beams Designed for Rapid Lesion Formation: Limitations Near the Skin During Multiple Lesion Treatments" (1997). Physics Publications and Research. Paper 26. http://digitalcommons.ryerson.ca/physics/26

This Conference Presentation is brought to you for free and open access by the Physics at Digital Commons @ Ryerson. It has been accepted for inclusion in Physics Publications and Research by an authorized administrator of Digital Commons @ Ryerson. For more information, please contact bcameron@ryerson.ca.

Authors JW Hunt, AY Xuan, E Seto, AE Worthington, L Chen, MC Kolios, and MD Sherar

NEW ACOUSTIC BEAMS DESIGNED FOR RAPID LESION FORMATION: LIMITATIONS NEAR THE SKIN DURING MULTIPLE LESION TREATMENTS**

J.W. HUNT, A.Y. XUAN, E. SETO, A.E. WORTHINGTON, L. CHEN, M.C. KOLIOS and M.D. SHERAR

** This work is supported by the National Cancer Institute of Canada

Research Department, Ontario Cancer Institute and Sunnybrook Hospital and Department of Medical Biophysics, University of Toronto, Toronto, Ontario M5G 2M9

Abstract - Minimally invasive surgery by intense focused ultrasound beams producing defined lesions is being studied extensively by different groups [1,2]. Lesion formation from a single pulse, depending on treatment time, tissue temperature [3], and pulse repetition of about 1 minute, should produce little damage near the skin. However, this scheme results in unacceptably long treatment times when used on larger tumors. A possible solution is to generate more rapid treatment times, or larger lesion volumes per pulse. However, hyperthermic temperatures in the overlying normal tissues including the skin may limit these treatments. In a previous presentation, simulations using an "ideal" transducer, pulses as short as 4 s and rapid stirring of the coupling bolus would reduce the temperature rise near the skin. Thus pulse repetitions as short of 10 s would be acceptable. However, real transducer beams show large aberrations which can greatly increase the near-field intensities, and make them unacceptable for hyperthermia therapy. Some artifacts are be caused by clamping of the transducer, others are related to thickness variations of the transducers which generate heterogenous phase shifts from different parts of the transducer which produce unwanted spreads at beam's focus. We will present detailed amplitude and phase scans near different transducers demonstrating the artifacts, and confirm them using ultrasound/magnetic-resonance phantoms showing the measured temperatures at the focus, and at 1 cm depth from the "skin" where the heating is considerably larger than that predicted by theory. Finally, we will discuss solutions for problems in the near field by improving the transducer mounting and reducing the unwanted phase shifts.

I. INTRODUCTION

An increasing number of centers are exploring the therapeutic potential of tissue lesion using focused ultrasound [1-7] The lesion diameter is best explained by hyperthermia response for the cells at the periphery of the lesion [3]. As described by extensive *in vitro* [8,9] and *in vivo* [10] studies, there is a nonlinear temperature/time response of hyperthermia. A relative thermal response above 43°C is best defined as equivalent thermal dose [11],

$$TD_{43} = \sum_{t=t_0}^{t} \frac{t_{end}}{t_{end}} 2^{T(t)-43} \Delta t \ge 42.5^{\circ}C$$
 (Min.), (1)

in which a treatment time (minutes) at a temperature T produces the same effects as at 43 °C. In this formulation, heating tissues for 120 min at 43 °C is the equivalent of treating at \sim 56 °C for a treatment of 1 sec, or 53 °C for 8 sec. Based upon the assessment by Kolios *et al* [3], a TD₄₃ of 60 min is considered to be sufficient to produce a lesion of defined diameter from 1 to 5 mm.

A serious limitation of high intensity focused ultrasound (HIFU) therapy is that large numbers of lesions are needed to "sterilize" the tumor. From experimental and theoretical evidence

[11,12], the pulse rate to form an array of lesions appears to be slow, i.e. 2 to 1/min. If one is treating a $3\times3\times3$ cm lesion producing lesions with a width of 0.2 cm, could take $(3/0.2)^2$ x 2 ~450 min. This would be an unacceptable treatment time. Thus different transducer designs such as cylindrical [13,14], conical [15], and multiple focused beams [16,17] are being considered to shorten the treatment times.

The aim of this paper is to explore the limitations for the temperatures reached near the skin during HIFU treatments. Because of the highly non-linear therapeutic response shown in equation (1), a short-lived, high temperature pulse appears to have considerable advantage over a continuous beam used near the patient's skin. Thus, to produce the same lesion size, if one shortens the pulse, the acoustic intensity must be increased to give a higher temperature. Because of the small lateral width of the focused beam, rapid cooling occurs due to thermal conductivity (main factor) and blood flow [18,3]. Near the skin, however, the diffused acoustic beam produces a much smaller temperature rise which cools more slowly. Thus a train of pulses produces an increasing temperature near the skin, and this is only acceptable if temperatures are kept below the therapeutic levels. Danuabiu and Hynynen [19] describe both theoretically and experimentally the special problems of lesion formation and optimizing certain parameters to limit their pulse repetition to two per minute.

This paper describes different treatment protocols and different optimizations that can be used, and practical limitations in the present treatment techniques. First, using an ideal spherical transducer, a simplified analysis is made of the heating and cooling of the lesion in the near field for multiple pulses. Second, a more accurate analysis was undertaken in which the beam distributions at different depths of the tissues were modeled using the bioheat transfer equation (BHTE) [20]. Third, an experimental evaluation of a "typical" transducer was undertaken to determine if experimental studies were in agreement with the theoretical studies. The latter is of considerable concern for air-backed transducers, since clamping the transducer to the holder can produce unwanted radial modes that can distort the acoustic distributions [21,22].

II. METHODS

A. Ultrasound field calculations

The details for the spherical and cylindrical transducers are shown in Table I and Figure 1(a). The beam distributions for a spherical transducer are well known, and are described in detail by Arditi et al [23]. This theory is valid for the system used by ter Haar and coworkers [18].

A cylindrical transducer is a potential alternative source, since a long, line lesion can be generated for a single pulse. The general design is shown in Figure 1(b). The beam distributions for a cylindrical transducer, studied by Foster et [14] for diagnostic imaging, were analysed using a modified conventional velocity potential approach,

$$p(r_1, \phi_1, t) = \frac{K}{j} \int_{-\phi/2}^{\phi/2} \frac{\exp[2\pi j(r/\lambda - vt)]}{r} r_2 d\phi_2 \quad ($$

where the complex continuous wave pressure field, $p(r_1, \varphi_1, t)$ is represented by the integral, K is the constant proportional to λ^{-1} , r_2 is the radius of the cylinder, r is the distance from the transducer to the point of observation, and ν is the frequency. The maximum pressure amplitude is $p_{max}(r_1) = Re_{max}p(r_1, \varphi_1, t)$. The trapezoidal rule was used to carry out a numerical integration for equations (2) and (3). Details are provided by Foster *et al* [13].

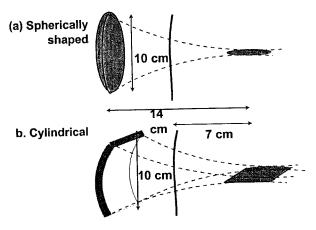


Figure 1. Two lesion designs compared for optimizing the lesion formation times. (a) Traditional spherically-shaped, air-backed transducer. (b) Cylindrical transducer producing a line-focus.

B. Temperature analysis

Two analyzes were made: one is a simplified analysis based upon the beam formation and cooling temperature profiles [3], while the second is a more accurate analysis using the BHTE.

1) Simplified Analysis: The simplified analysis based upon the initial cooling rate at the focus, and at the skin, can be approximated by

$$dT/dt = I - kT, (4)$$

while the formation of the temperature growth is given by

$$T_{t} = \frac{I}{k} - C e^{-kt} \tag{5}$$

where T is the excess temperature, I is the heating rate (°C/s) and k_f and k_s are first order rates (s¹) at the focus, and at the skin. Note the large differences in values used are shown in Table I. Note that inside a large treatment field, $k_s \approx w_b$.

Since multiple focused beams are needed to effectively treat the complete tumor, a slow increase in temperature during the treatment is seen: the mathematical analysis is similar for pulseradiolysis [23]. The effects due to surface cooling were not considered. Figure 2 shows the growth for a pulse repetition rate/minute of 1.0.

2) More complete temperature calculations: A finite difference algorithm was used to solve the BHTE analysis in cylindrical coordinates [3]. The boundaries are the skin at 7 cm from the focal length, 14 cm., and assume that there is rapid stirring, uniform tissue properties are constant, and the tissue volume such that there are no thermal gradients due to for side and back boundaries. In all cases, we assume the same lesion diameter (Table 1), based upon the same $TD_{43} = 60$ min. for the spherically-shaped and cylindrical transducer. Note that with a shorter pulse length, using the same TD_{43} , both the acoustic power and temperature must be increased to obtain the same lesion diameter.

TABLE 1. PARAMETERS USED IN THE SIMULATION					
Initial cooling rate (k _r) at the focus (s ⁻¹)	0.29	Frequency (MHz)	1.7		
Initial cooling rate (k _s) near the skin (s ⁻¹)	0.003	Transducer radius of curvature (cm)	14		
Skin surface-to transducer distance (cm)	7	Transducer diameter (cm)	10		
Interval between pulses (s)	60	Intensity absorption coefficient (Np/cm)	0.2		
Lesion diameter (mm)	2	Attenuation coefficient (Np/cm)	0.2		
Uniform geometrical intensity at the skin (cm)	5	Blood mass perfusion w _b (g/cm ³ /s)	0.003		
Tissue specific heat, C (J/g/°C)	4.18	Tissue and blood density ρ _t (g/cm³)	1.00		

C. Experimental Design:

- 1) Transducer Acoustic Distributions: The acoustic distributions were measured by a PVDF hydrophone with an active diameter of 0.84 mm and scanned over a 40×40 mm field. A fairly short burst (60 cycles) and absorbing acoustic dump were used to reduce unwanted artifacts. To confirm that unusual results were not due to artifacts, the transducer was rotated along the axis by 90°.
- 2) Magnetic Resonance Images: A new phantom, made of polyethylene glycol (PEG)/polyacrylamide (PA) gel, was developed in our laboratory. It has an attenuation of 0.95 ± 0.4 dB @ 10 MHz, and no loss of sensitivity for MRI analysis. The temperature measurements were carried out using a commercial 2D fast spoiled gradient-echo sequence (SPGR), in which the 1 H proton resonance-shift method mainly measures the ratio between the hydrogen-bonded and non-bonded water molecules.

III. RESULTS

A. Predicted Temperature Increase in the Near Field

1) Spherically-Shaped Source: The goal is to compare the theoretical and experimental intensities and distributions at the focus, and in the near field. Figure 2 shows the predicted isothermal curves from focused beams just after 4 and 16 s pulses. Details of the parameters used are given in Table 1. Note the very small temperature increase predicted just inside the skin for the 4 s pulse, and particularly the effective surface cooling. Figure 3 shows the building of the temperature increase for a continuous acoustic source, and four pulse lengths, 16, 12, 8, and 4 s for a spherically-shaped transducer. The left panel in Figure 2 shows the temperature growth of the heating and cooling analysis for a repetition rate of 1

pulse/min, while the solid lines are based upon the more accurate cooling rates at the lesion, and at the skin. The right panel in Figure 2 shows a more complete analysis using a finite difference algorithm to solve the BHTE in a homogeneous tissue model [3]. This model includes a cooling water bolus at the surface of the skin. Note that both models show large improvements for the temperatures reached by using the shortest pulses. This is mainly due to the rapid cooling of the small lesion diameters.

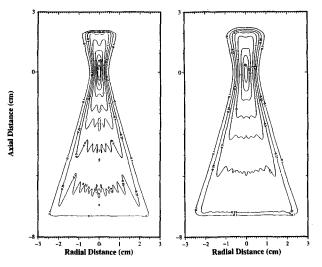


Figure 2. The isothermal temperatures for a 4 s pulse (left), and 16 s pulse (right) cooling produced by the spherically-shaped transducer.

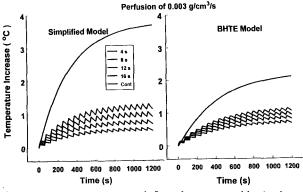
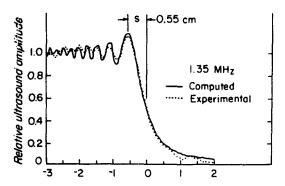


Figure 3. The temperature growth for pulses separated by 1 min. and designed to produce the same lesion sizes. The simplified model (left) is based upon the cooling rates, k_f at the focus, and k_s at the skin, while the right is the more accurate analysis using the BHTE model, and assuming unstirred water cooling at the skin. At a depth of 5 cm , the temperature profiles are similar.

(2) Cylindrical Transducer. The same criteria was used for the lesion formation as for the spherically shaped transducer. The special property is the sharp boundary or the line focus produced by a cylindrical transducer (Fig. 4). Figure 5 shows the development of the temperature distribution immediately after 4 s and 30 s after a 4 s pulse. This shows the very high temperature at the therapeutic levels even 30 sec after the pulse at 5 mm depth in the body.



Distance from the edge of the line focus (cm)

Figure 4. The theoretical and experimental distribution of line -focus showing the rapid cutoff from the beam that has the potential advantage to better delineate tumor boundaries. From Foster *et al.*[13].

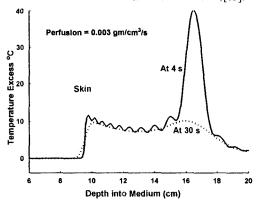


Figure 5. The simulated heating profiles from a cylindrical transducer with rapid cooling at the skin boundary set at 0°C for immediately after a 4 s, and at 30 s.

B. Experimental Distributions Produced by a Spherical Transducer.

(1) Distributions at the focus and in the near field. The simulations for a spherically-shaped transducer suggest that temperatures reached near the skin should be low. Practically, higher temperatures near the skin have been observed. One possible problem could be the very high absorption of the skin. Another possibility is that the air-backed transducer used for the treatments does not follow the theories of an unclamped transducer, and instead produces unwanted modes which can reduce the efficiency of concentrating most of the beam at the focus. To study this, we used a transducer currently used successfully for lesion formation studies.

Figure 6 shows one of the artifacts produced for a clamped 10 cm diameter, 1.7 MHZ PZT4 transducer focused at 10 cm. The experimental arrangement is described in the Methods section. The distribution at 5 cm from the transducer is shown. Note the two overlapping patterns that are likely due to radial resonances formed by clamping and sealing the PZT4 transducer to the water coupling. In addition, the predicted FWHM of the beam at the focus is 1.3 mm in comparison to the observed FWHM of 2.5 mm, thus a correction is made for larger area.

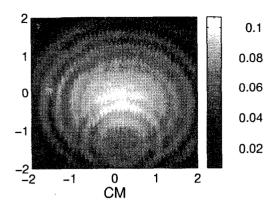


Figure 6. Observed acoustic distribution at a distance of 5 cm from the transducer. Note the two overlapping distributions which indicate a defect in the holder for the transducer.

(2) The acoustic intensity and heating at the focus, and in the near field. The observed "skin"/peak ratio, S/P, for the intensity was summarized in Table 1. The observed S/P is ~ 2.4 greater than expected from theory.

Table 2						
Beam Properties	FWHM mm	Observe S/P	Corrected S/P Ratio			
Theoretical	1.3	0.0004	0.00040			
Observed	2.5	0.0035	0.00095			

In addition, the preliminary studies using the MRI phase-shift technique for a 100 s heating, a temperature increase at the focus was 32±2°C, and at 5 cm from the transducer (position of the skin) the temperature was 6±4°C. While these temperature experiments cannot be compared directly for much shorter pulses, it supports the evidence that a much larger S/P ratio has been observed than predicted by theory.

IV. DISCUSSION AND CONCLUSION

One of the limitations of HIFU systems used for minimal invasive surgery is the time needed to treated a malignant tumor. As shown from simulations described in this paper using "ideal" transducer beams, the beam in the near field, i.e., near the skin, only a small temperature increase is predicted for a single pulse, since a series of pulses are needed. As noted in Figures 2 & 3, for an ideal spherically-shaped source and a short pulse (4 s), the temperature increase reached should be less than 0.5°C.

The experimental data for the defective transducer shown here shows a factor 2.4 times greater than predicted. This predicts skin temperatures should reach therapeutic temperatures for repetitive pulses. Thus we recommend that each transducer should be checked for the near field distribution and intensity ratios before being used for clinical studies. Other factors such as higher acoustic absorption in the skin must be considered.

The simulations for an ideal cylindrical transducer, which spreads the acoustic field in a long line focus, shows that the S/P temperature ratio is ~25%, and suggest that a single pulse can produce enough energy in the skin that a significant thermal dose might occur. However, since it produces a better defined treatment field, it would still be useful if one allowed a longer treatment time.

REFERENCES

 G. ter Haar, D., Sinnett, and I. Rivers, "High intensity focused ultrasound -- a surgical technique for the treatment of discrete liver tumors," *Phys. Med. Biol.* vol. 34, 1743-1750, 1989.

- [2] K. Hynynen, A. Darkazonli, and E. Unger, "MRI-guided noninvasive ultrasound surgery," Med. Phys. vol. 20 107 - 115, 1993.
- [3] M.C. Kolios, M., M.D. Sherar, and J.W. Hunt. "Blood flow cooling and ultrasonic lesion formation." *Medical Physics*, vol 23 (7), 1287-1298, 1996
- [4] W. Fry and F. Fry, "Fundamental neurological research and human neurosurgery using intense ultrasound," *IRE Transactions in Medical Electronics*, vol ME-7, 166-181, 1960.
- [5] P.P. Lele, "Production of deep focal lesions for focused ultrasound current status," *Ultrasonics*" vol.5, 105-122. 1962.
- [6] C.R., I.Rivers, M.G. Vaughan, and G.R. ter Haar, Lesion development in focused ultrasound surgery: A general model," J. Ultrasound in Med. Biol. vol. 20, 259-269, 1994.
- [7] L. Chen, I. Rivers, G. ter Haar, S. Riddler, C.R. Hill, and J.P. Bensted, "Histological changes in rat liver tumours treated with high-intensity focused ultrasound," J. Ultrasound in Med. and Biol, vol. 19, 67-74, 1993.
- [8] S.A. Separeto and W.C. Dewey, "Thermal dose determination in cancer therapy," Int. J. Radiation Oncology, Biol. and Phys., vol. 10, 787-800, 1984.
- [9] J.L. Borelli, L. Thompson, C.C. Cain, and W.C. Dewey. "Time-temperature analysis of cell killing of BHK cells heated at temperatures in the range of 43.5 C to 57.0 C," Int. Jr. of Radiation Oncology, Biol. & Phys. vol. 19, 389-399, 1990.
- [10] S.B. Field and C.C. Morris, "The relationship between heating time and temperature: its relevance to clinical hyperthermia," *Radiotherapy and Oncology* vol. 1, 179-186, 1980.
- [11] C. Damianou and K. Hynynen, "The effect of various physical parameters on the size and shape of necrosed tissue volume during ultrasound surgery," J. Acoust. Soc. Am., vol. 95, 1641-1649, 1994.
- [12] N.A. Watkin, G. R. ter Haar, and I. Rivens, "The intensity dependence of the site of maximal energy deposition in focussed ultrasound surgery". *Ultrasound in Med. & Biol.* vol. 22 (4), 483-491, 1996.
- [13] F.S. Foster, M. Arditi, and J.W. Hunt, "Cylindrical transducer scatter-scanner", Jr. Acoustic Soc. of America, vol. 68, 85-95, 1980.
- [14] E.S. Ebbini, S. Umemura, M. Ibbini, and C.A. Cain, "A cylindrical-section ultrasound phased-array applicator for hyperthermia cancer therapy," IEEE Trans. *Ultrason. Ferroelectr. Freq. Contr.* vol 35, 561-572, 1988.
- [15] F.S. Foster, M.S. Patterson, M. Arditi., and J.W. Hunt, "The conical scanner: A two transducer ultrasound scatter imaging technique," *Ultrasonic Imaging*, vol 3, 62-82, 1981.
- [16] X. Fan and K. Hynynen, "A study of various parameters of spherically curved phased arrays for noninvasive ultrasound surgery," *Phys. Med. Biol.* vol. 41, 591-608, 1996.
- [17] R.J. Lalonde, J.W. Hunt, "Optimizing ultrasound focus distributions for hyperthermia," *Transactions in Biomedical Engineering*, vol. 42, 981-990, 1995.
- [18] L. Chen, G. ter Haar, C.R. Hill, M. Dworkin, P. Carnochan, H. Young, and J.P. Bensted, "Effects of blood perfusion on the ablation of liver parenchyma with high-intensity focused ultrasound," *Phys. Med. Biol.*, vol 38, 1661-1673, 1993.
- [19] C. Damianou, and K. Hynynen, Focal spacing and near-field heating during pulsed high temperature ultrasound therapy. *Ultrasound in Med.* & Biol, vol. 19, 777-787, 1993.
- [20] H.H. Pennes, "Analysis of tissue and arterial blood temperatures in the resting human forearm", J. Appl. Physiol, vol. 1, 93-122, 1948.
- 21] P. Monro, R.P. Hill and J.W. Hunt, "The development of improved ultrasound heating suitable for superficial tissue heating". *Med. Phys.* vol. 9, 888-897, 1982.
- [22] G. Harrison, "Ultrasound hyperthermia applications: Intensities distributions and quality assurance", Int. Jr. Hyperthermia, vol. 6, 169-174, 1990.
- [23] M. Arditi, J.F. Foster and J.W. Hunt, "Transient fields of concave annular arrays," *Ultrasonic Imaging* vol. 3 (1), 37-61, 1981.
- [24] M.J. Bronskill, R.K. Wolff, and J.W. Hunt, "Picosecond pulse radiolysis studies. I. The solvated electron in aqueous and alcohol solutions," Jr. Chem. Phys. vol. 53, 4201-4210, 1970.